



20 1 Introduction

21 With a total land area of about 1100 km², Hong Kong is one of the most densely populated regions in
22 the world with a population of about 7.5 million (GovHK, 2019). Throughout the territory of Hong
23 Kong, there are more than 57, 000 registered man-made slope features (Cheung and Tang, 2005).
24 With an average annual rainfall of about 2400 mm, rainfall induced landslides are one of the major
25 natural hazards threatening the public safety in Hong Kong (GEO, 2017). In particular, slope failures
26 along highways have resulted in serious fatalities, damaged vehicles and disruption to the traffic. For
27 example, in August 1994, a public light bus on the Castle Peak Road was hit by landslide debris,
28 causing three persons trapped inside the bus and one man killed. In August 1995, the slope along
29 Shum Wan Road failed, induced by large rainfall, which resulted in two fatalities and five injuries. In
30 August 1997, the landslide along Ching Cheung Road resulted in the closure of the highway for more
31 than three weeks (GEO, 2017). Similar phenomena have indeed also been reported in many other
32 parts of the world (Bil et al., 2015), such as Italy (Donnini et al., 2017) and India (Negi et al., 2013).

33 There are many uncertainties in the assessment of the hazard of moving vehicles hit by
34 **and what about the probability that the sliding mass reaches the road??**
35 landslides, such as the occurrence of landslides, the travel distance of the landslide and the presence
36 of the moving vehicles at the moment of landslides. Risk assessment is a framework in which both
37 the uncertainties and the consequence of a hazard can be addressed, which is now increasingly been
38 used for landslide risk management (e.g. Lessing et al., 1983; Fell, 1994; Dai et al., 2002; Remondo
39 et al., 2008; Erenner, 2012; Vega and Hidalgo, 2016). Indeed, landslide risk assessment has been
40 accepted as an effective tool for the planning of land use in Hong Kong. Nevertheless, the risk
41 assessment of moving vehicles **affected** **attacked** by landslides is special **because** **in that** the elements at risk are highly
mobile. Several studies have also been conducted on assessing the impact probability of landslides



42 on vehicles (e.g. Budetta, 2004; Peila and Guardini, 2008; Nicolet et al., 2016). Fell et al. (2005)
43 assessed the probability of a falling block hitting a vehicle based on the length of the vehicle and the
44 traffic flow. Dorren et al. (2009) suggested a method to assess the probability of a vehicle hit by a
45 landslide based on the dimension of the landslide and the traffic flow. Michoud et al. (2012) assessed
46 the probability of a vehicle hit by a falling rock considering the dimensions of the vehicle and size of
47 falling rocks. However, few attempts have been made to suggest a rigorous assessment framework of
48 vehicles hit by landslides. As such, implementation of rigorous risk assessment of vehicles hit by
49 landslides is still challenging.

50 Through a case study in Hong Kong, the objective of this paper is to suggest a method to
51 quantitatively assess the risk of vehicles hit by landslides along highways. The structure of this paper
52 is as follows. Firstly, **the annual failure probability of the slope is calculated**. Then,
53 the spatial impact of the landslide is analyzed. Thereafter, the consequence of the landslide is
54 analyzed. Finally, the annual risk of vehicles hit by the landslide is calculated. **The assessment**
55 **method provides a convenient and useful tool to investigate the risk of vehicles hit by landslides in**
56 **Hong Kong.**

¿How is possible to get that the suggested method be adaptable to others territories?

57

58 **2 Engineering Background**

It will be more proper. particular conditions of case study or something like that..

59 Fig. 1 shows the slope under investigation in this study, which is along the Kennedy Road in the Wan
60 Chai district of Hong Kong. Wan Chai is one of the oldest and most traditional cultural areas in Hong
61 Kong and attracts many tourists. According to Transport Department of Hong Kong (TDHK) (2018),
62 Kennedy Road is a major road with three lanes in this region. Fig. 2 shows a typical cross section of
63 the slope. **Fig. 2 says 25m.... Include this value in Fig 2.** The height of the slope, H , is 26 m and the slope angle is about 45 degrees. As shown in

This section should provide to reader some information about geological & geotechnical conditions of the slope with the aim to introduce him in the slope stability concepts



64 this figure, the horizontal distance from the crest of the landslide scar to the side of Kennedy Road
65 close to the slope, l_{ch} , is about 35 m and the horizontal distance from the slope toe to the side of
66 Kennedy Road close to the slope, l_{th} , is about 3 m. The width of Kennedy Road, b_h , is 10 m. Fig. 3
67 shows the plan view of the slope. The landslide scar is about 25 m in length and about 18 m in width.

68 **This phrase should be in the begin of this section.**
68 On 8 May 1992, the slope failed during an intense rainfall, which hit a car travelling along Kennedy
69 Road and killed the driver (GEO, 1996). According to TDHK (2018), vehicles in Hong Kong are
70 composed of private buses, non-franchised public buses, franchised buses, taxis, private cars, public
71 light buses, private light buses, goods vehicles, special purpose vehicles, government vehicles and
72 motor cycles. The percentage of each type of vehicle with respect to total numbers of vehicles is
73 shown in Table 1 (TDHK, 2018). According to TDHK (2018), the typical length of each type of
74 vehicle is also shown in Table 1. The purpose of this case study is to analyze the risk of vehicles hit
75 by the landslide if this slope fails again.

76

77 **3 Methodology**

78 In general, the risk of a landslide hazard depends on the likelihood of the landslide, the spatial extent
79 of the landslide and the number of vehicles being hit by the landslide. There are multiple types of
80 vehicles on a highway. **In a landslide critical zone of the road, the longer...**
81 landslide. Let $P(F)$ denote the annual probability of slope failure. Suppose there are m possible
82 spatial impacts and let $P(\mathbf{S} = \mathbf{S}_i | F)$ denote the chance that the spatial impact is \mathbf{S}_i when the landslide
83 occurs. Let $P(n_j = k | \mathbf{S} = \mathbf{S}_i)$ denote the chance that the k type ^{of} j vehicle will be hit by the landslide
84 when the spatial impact is \mathbf{S}_i . The risk associated with the j th type of vehicle, i.e., the expected
85 annual number of type j vehicles being hit by the landslide, can be calculated as follows:



It is not possible 0 spatial impacts? and then, $i=0$

$$R_{vj} = P(F) \times \sum_{i=1}^m \left[P(\mathbf{S} = \mathbf{S}_i | F) \times \sum_{k=1}^{\infty} kP(n_j = k | \mathbf{S} = \mathbf{S}_i) \right] \quad (1)$$

are there infinite value for types of vehicles?

Let n_v denote total types of vehicles. The total risk of vehicles hit by the landslide considering all types of vehicles, i.e., R_v , can then be calculated as follows:

$$R_v = \sum_{j=1}^{n_v} R_{vj} \quad (2)$$

Let n_{pj} denote the average number of persons in a type j vehicle. The risk of people hit by the landslide can be calculated as follows:

$$R_{pj} = P(F) \times \sum_{i=1}^m \left[P(\mathbf{S} = \mathbf{S}_i | F) \times \sum_{k=1}^{\infty} kP(n_j = k | \mathbf{S} = \mathbf{S}_i) \right] \times n_{pj} \quad (3)$$

The total risk of people hit by the landslide considering all types of vehicles can be calculated as follows:

$$R_p = \sum_{j=1}^{n_v} R_{pj} \quad (4)$$

As can be seen from the above equations, the keys for risk assessment are to evaluate: (1) the annual failure probability of the landslide, i.e., $P(F)$, (2) the spatial impact of the landslide, i.e., $P(\mathbf{S} = \mathbf{S}_i | F)$ and (3) the number of vehicles being hit by the landslide for a given spatial extent, i.e., $P(n_j = k | \mathbf{S} = \mathbf{S}_i)$. How the above elements are assessed is introduced in the following sections.

It should not be sufficient only a slope failure, because the sliding mass might not reach the road, even a vehicle. Why? because that probability of reach de road depends of slope geometry, geotechnical parameters, etc... then how you could explain and include this consideration in your model?

3.1 Evaluation of annual probability of the landslide, $P(F)$

The estimation of the probability of occurrence of landslides within a given period of time is fundamental in landslide hazard assessment. Since almost slope failures in Hong Kong are caused by rainfall infiltration (e.g. Lumb, 1975; Brand, 1984; Finlay et al., 1999), assessing annual probability of rainfall-induced landslides is important. In general, there are two types of methods for evaluating



106 **physically-based models**
the likelihood of slope failure within a given exposure time: methods through slope stability analysis
107 built on principles of soil mechanics (e.g. Christian et al., 1994; Fenton and Griffiths, 2005; Huang et
108 al., 2010) and empirical methods through statistical analysis of historical slope failure data (e.g. Chau
109 et al., 2004; Tang and Zhang, 2009). Currently, landslide probability analyses via slope stability
110 analyses mainly focus on the likelihood of slope failure for a given rainfall. As an illustration, the
111 statistical methods are used to estimate the annual landslide probability. **or landslide susceptibility.**

112 In Hong Kong, the failure of a slope is highly correlated to the 24-hour rainfall, i_{24} (Cheung and
113 Tang, 2005). Zhang and Tang (2009) divided the rainfall events in Hong Kong into three categories
114 based on i_{24} , i.e., (1) $i_{24} < 200$ mm/day (small rainfall, denoted as *SR*), (2) $200 \text{ mm} < i_{24} < 400$
115 mm/day (medium rainfall, denoted as *MR*) and (3) $i_{24} > 400$ mm/day (large rainfall, denoted as *LR*).

116 Based on slope failure data observed in Hong Kong during 1984-2002, it is found that the failure
117 probability of an average slope in Hong Kong when subjected to small rainfall, medium rainfall and
118 large rainfall is 1.09×10^{-4} , 2.61×10^{-3} and 8.94×10^{-3} , respectively (Zhang and Tang, 2009), i.e.,
119 $P(F|SR) = 1.09 \times 10^{-4}$, $P(F|MR) = 2.61 \times 10^{-3}$ and $P(F|LR) = 8.94 \times 10^{-3}$. The above analyses
120 provide the conditional failure probability of a slope for a given type of rainfall. To evaluate the
121 annual probability of slope failure, the probability of each type of rainfall should be analyzed. For
122 such a purpose, Fig. 4 shows the histogram of the yearly maximum i_{24} measured at Hong Kong
123 Observatory Headquarters during 1969 and 2018 (HKO, 2018). As can be seen from Fig. 4, the
124 maximum i_{24} in a year in Hong Kong is mainly in the range of 100 to 350 mm. The generalized
125 extreme value distribution (Hosking et al., 1985) with the following probability density function
126 (PDF) seems to fit the histogram with reasonable accuracy:



$$f(i_{24}) = \frac{1}{\beta} \left[1 + \gamma \left(\frac{i_{24} - \mu}{\beta} \right) \right]^{-\frac{1}{\gamma}} \exp \left\{ \left[1 + \gamma \left(\frac{i_{24} - \mu}{\beta} \right) \right]^{-\frac{1}{\gamma}} \right\} \quad (5)$$

where β , μ and γ are the scale parameter, the location parameter and the shape parameter of the generalized extreme distribution, respectively. The values of β , μ and γ can be calculated based on maximum likelihood method and they are equal to -0.17, 66 and 188, respectively. Fig. 5 shows the cumulative distribution function (CDF) of i_{24} obtained based on the fitted generalized extreme value distribution. As can be seen from this figure, the probability that the rainfall with yearly maximum i_{24} belongs to small rainfall, medium rainfall and large rainfall is 0.44, 0.55 and 0.01, respectively, i.e., $P(SR) = 0.44$, $P(MR) = 0.55$ and $P(LR) = 0.01$. Based on the total probability theorem, the annual probability of slope failure can be computed as follows:

$$P(F) = P(F | SR) P(SR) + P(F | MR) P(MR) + P(F | LR) P(LR) \quad (6)$$

3.2 Evaluation of spatial impact of the landslide, $P(S = S_i | F)$

and indeed it has a probability ...
The spatial impact of a landslide depends on whether the landslide can reach the highway and the length of the affected road if the landslide can reach the highway. In general, methods to investigate the travel distance of a landslide can be divided into two categories (Hung et al., 2005), i.e., (1) analytical or numerical methods based on the physical laws of solid and fluid dynamics (Scheidegger, 1973), which are often solved numerically (e.g. Hung and McDougall, 2009; Luo et al., 2019) and (2) empirical methods based on field observations (e.g. Budetta and Riso, 2004; Dai and Lee, 2002). and geometric correlations
Since the empirical method is more convenient to apply (Finlay et al., 1999), it is used in this paper. As illustrated in Fig. 2, the travel distance of the sliding mass (L) is highly related to the volume (V) and height (H) of sliding body (e.g. Corominas, 1996; Liang et al., 2017). According to historical and geotechnical, hydraulic and rheological properties of sliding mass



148 data in Hong Kong, Corominas (1996) found that the travel distance of landslide debris can be
149 estimated using the following equation: in landslide debris is important water content
of sliding mass and geometry slope

$$150 \quad \log L = 0.085 \log V + \log H + 0.047 + \varepsilon \quad (7)$$

151 where ε is a random variable with a mean of zero and a standard deviation of $\sigma = 0.161$.

152 For the slope as shown in Fig. 2, the height is 25 m, i.e., $H = 25$ m. To apply Eq. (7), the
153 landslide volume is needed. Let A_s denote the landslide scar area, which can be related to landslide
154 volume through empirical relationships (e.g. Malamud et al., 2004; Imaizumi and Sidle, 2007;
155 Guzzetti et al., 2008; Guzzetti et al., 2009). In this study, the power relationship suggested by Parker
156 (2011) is used: This formulation is aplicable for back analysis because you know
landslide scar, but for not ocurred events?

$$157 \quad V = 0.106 \times A_s^{1.388} \quad (8)$$

158 Based on Fig. 3, the landslide scar area is estimated to be 450 m². Based on Eq. (8), the volume
159 is estimated about 510 m³, Which was the real value? which is close to the real volume of sliding mass in the landslide event on
160 8 May 1992 (GEO, 1996). Substituting the values of H and V into Eq. (7), it can be obtained that the
161 travel distance of the landslide is lognormally distributed with a mean of 50.7 m and a standard
162 deviation of 12.6 m. Fig. 6 shows the PDF of the travel distance of the landslide. As can be seen from
163 this figure, the value of travel distance of the landslide is mainly in the range of 20 m to 150 m.

164 The spatial extent of the landslide is also related to the length of the affected road. As shown in
165 Fig. 3, when the head or the rear of a vehicle contacts with the landslide mass, the vehicle will be hit
166 by the landslide, i.e., the number of vehicles being hit by landslides depends on the width of the
167 landslide (b_l) and the length of the vehicles (l_v). The length of affected road, l_a , is the sum of the
168 width of the landslide and the length of vehicles, i.e.,

$$169 \quad l_a = b_l + 2l_v \quad (9)$$



170 In this study, the spatial extent of the landslide is characterized by the length of the affected road
 171 **This term should be defined earlier to introduce to reader in this terminology**
 171 and the **runout distance** of the landslide, i.e., $S = \{l_a, L\}$. For simplicity, the uncertainty associated
 172 with the length of the affected road is not considered. In such a case, the uncertainty associated with
 173 S is fully characterized by the uncertainty associated with the runout distance. In principle, the runout
 174 distance is a continuous random variable. For simplicity, it can be discretized into a discrete variable.
 175 Let L_i denote the i th possible value of L and let $S_i = \{l_a, L_i\}$. $P(S = S_i | F)$ can be calculated by

$$P(S = S_i | F) = P(L = L_i) \quad (10)$$

177

178 3.3 Evaluation of encounter probability, $P(n_j = k | S = S_i)$

179 As shown in Fig. 2, the horizontal distance from the crest of the landslide scar to the side of Kennedy
 180 Road close to the slope is about 35 m, i.e., $l_{ch} = 35$ m. The width of Kennedy Road is about 10 m, i.e.,
 181 $b_h = 10$ m. The landslide will reach Kennedy Road once $L > l_{ch}$. When $L \geq l_{ch} + b_h$, the Kennedy Road
 182 will be totally covered by the sliding mass. When $l_{ch} < L < l_{ch} + b_h$, the Kennedy Road will be
 183 partially affected. Thus, the **percent?** **proportion of vehicles** within the affected length of the Kennedy Road
 184 which will be hit by the landslide, denoted as $\alpha(S = S_i)$ here, can be calculated as follows:

$$\alpha(S = S_i) = \begin{cases} 0, & L_i \leq l_{ch} \\ \frac{L_i - l_{ch}}{b_h}, & l_{ch} < L_i < l_{ch} + b_h \\ 1, & L_i \geq l_{ch} + b_h \end{cases}$$

This relation can be produce fractional numbers....
 which is the meaning (of) these values in the context of vehicles number?? It is an affectation degree?

186 In general, the number of vehicles hit by landslides highly depends on the density of vehicles,
 187 the spatial extent of the landslide and the size of the vehicles. The presence of the vehicles on a
 188 highway can be modeled as a Poisson process with a mean arrival rate of λ (Paxson and Floyd, 1995).
 189 Let q denote the number of vehicles passing a given cross section of a road per unit time. Let v



190 denote the average speed of the vehicles. The mean rate of occurrence of moving vehicles, λ , can be
191 calculated as follows (Lighthill, 1995):

$$192 \quad \lambda = \frac{q}{v} \quad (12)$$

193 Let w_j denote the proportion of type j vehicle in the traffic flow. The mean rate of occurrence of
194 type j vehicle can be then written as follows:

$$195 \quad \lambda_j = w_j \times \frac{q}{v} \quad (13)$$

196 As an example, Table 2 shows the data about q and v of the Kennedy road for the morning peak,
197 normal period and evening peak, respectively, which are obtained from TDHK (2018). As shown in
198 Fig. 3, the width of the landslide is about 18 m, i.e., $b_l = 18$ m. The length of each type of vehicle, l_j ,
199 are shown in Table 1. Based on these data, the mean rate of occurrence of each type of vehicle can be
200 calculated for different periods of a day, as shown in Figs. 7(a)–(c), respectively. It can be seen that
201 the mean rate of occurrence of the vehicles during the morning and evening peak is significantly
202 larger than that in the normal period. Among all types of vehicles, the mean rate of private cars in the
203 affected road is the greatest, followed by goods vehicles, motor cycles and taxis.

204 Let T_1 , T_2 and T_3 denote the morning peak, the normal period and the evening peak, respectively;
205 and l_{aj} denote the length of affected road for type j vehicle. Based on the property of a Poisson
206 process, if the spatial impact is $\mathbf{S} = \mathbf{S}_i$ and the slope fails during period T_i , the chance that k type j
207 vehicles will be hit by the landslide can be computed by

$$208 \quad P(n_j = k \mid t \in T_i, \mathbf{S} = \mathbf{S}_i) = \frac{[\alpha_j(\mathbf{S} = \mathbf{S}_i) \lambda_j l_{aj}]^k}{k!} \exp[-\alpha_j(\mathbf{S} = \mathbf{S}_i) \lambda_j l_{aj}] \quad (14)$$

209 As an example, Figs. 8(a)–(c) shows the distributions of the number of private cars hit by the
210 landslide for the case of $\alpha_j(\mathbf{S} = \mathbf{S}_i) = 1$ when the slope failure occurs during the morning peak, normal



211 period and evening peak, respectively. As can be seen from these figures, the most probable number
212 of private cars hit by the landslide when the slope failure occurs during the morning peak and
213 evening peak is both about 3 and its probability is both about 0.20. The most probable number of
214 private cars hit by the landslide when the slope failure occurs during the normal period is about 1 and
215 its probability is about 0.37.

216 In Eq. (14), the failure time is assumed known. In reality, the slope can fail during any period of
217 a day. Based on the total probability theorem, the probability that k Type j vehicles will be hit for the
218 case of $\mathbf{S} = \mathbf{S}_i$ can be computed by

$$219 \quad P(n_j = k | \mathbf{S} = \mathbf{S}_i) = \sum_{i=1}^3 P(n_j = k | t \in T_i, \mathbf{S} = \mathbf{S}_i) P(t \in T_i) \quad (15)$$

220 As an example, Figs. 8(d) shows the probability distribution of the number of private cars hit by
221 the landslide for $\alpha_j(\mathbf{S} = \mathbf{S}_i) = 1$ considering the uncertainty of the failure time. As can be seen from
222 this figure, the most probable number of private cars hit by the landslide considering the uncertainty
223 of the failure time is about 1 and its probability is about 0.32.

224

225 3.4 Risk assessment

226 In the above analyses, equations for evaluating $P(F)$, $P(\mathbf{S} = \mathbf{S}_i | F)$ and $P(n_j = k | \mathbf{S} = \mathbf{S}_i)$ are introduced.
227 Substituting these equations into Eq. (1), the risk of each type of vehicles hit by the landslide studied
228 in this paper can then be calculated, which are shown in Figs. 9(a). As can be seen from this figure,
229 the annual risk of private cars hit by the landslide is the greatest with a value of 1.67×10^{-3} vehicles
230 **In economic or monetary terms... which the value of potential losses?** per year, followed by the goods vehicles, motor cycles and taxis. The risk associated with each type

231 of vehicle is highly correlated with the proportion of vehicles in the traffic flow. The private cars
232 have the greatest proportion in the traffic flow and hence it is natural to be associated with the

It is suggested to comment if these values correspond to high or low risk values according some risk scale



233 greatest risk. In reality, the vehicle that was hit by the studied slope on 8 May 1992 was indeed a
234 private car. With Eq. (2), the risk of vehicles hit by the landslide considering all types of vehicles can
235 be also calculated, which is about 2.48×10^{-3} vehicles per year.

236 The passenger capacity of each type of vehicle can be investigated through TDHK (2018) and
237 the assumed average number of persons in a vehicle is also shown in Table 1. Submitting these
238 numbers into Eq. (3), the risk of persons hit by the landslide associated with each type of vehicle can
239 be computed and the results are shown in Figs. 9(b). As can be seen from this figure, the annual risk
240 of persons hit by the landslide for private cars is the greatest with a value of 8.37×10^{-3} persons per
241 year, followed by non-franchised public buses, franchised buses and goods vehicles. The risk to
242 persons for each type of vehicles highly depends on the proportion of vehicles in the traffic flow and
243 the passenger capacity of vehicles. The non-franchised public buses have the higher proportion in the
244 traffic flow and the largest passenger capacity hence it is natural to be associated with the greater risk.
245 Based on Eq. (4), the risk of persons hit by the individual landslide studied in this paper considering
246 all types of vehicles can be also calculated, which is about 1.36×10^{-2} persons per year.

247

248 **4 Discussions**

249 **4.1 Effect of annual failure probability of the slope**

250 In the above analysis, the annual failure probability of the slope is 1.58×10^{-3} , which is calculated
251 based on historical data in Hong Kong and represents the failure probability of an average slope in
252 **under which considerations??** Hong Kong. To investigate the effect of the failure probability of the slope, Fig. 10 shows the annual
253 risk of the slope calculated based on different annual failure probabilities. As can be seen from this
254 figure, the annual risk to all types of vehicles increases linearly with the annual failure probability of



255 the slope. When the failure probability of the slope increase from 1.0×10^{-4} to 1.0×10^{-2} , the annual
256 risk to vehicles increases from 1.57×10^{-4} vehicles being hit per year to 1.57×10^{-2} vehicles being hit
257 per year. A similar observation can also be found for the annual risk to persons. Hence, reducing the
258 annual failure probability of a slope is an effective means to reduce the risk of the slope.

do you suggest some kind of measures to reduce the AFP & that it can be consider in your model?

259

What about geotechnical properties of soil and slope geometry that
favor that the sliding mass reaches the road?

260 4.2 Effect of distance from the slope to the highway

and the economics losses, too!

261 The risk of damaged vehicles due to landslides is highly associated with spatial impact of landslides.

262 The further the road is away from the slope, the less chance the road will be affected by the slope. In

263 the above analysis, the horizontal distance from the crest of the landslide scar to the side of Kennedy

264 Road close to the slope, l_{ch} , is about 35 m and the horizontal distance from the slope toe to the side of

265 Kennedy Road close to the slope, l_{th} , is about 3 m (GEO, 1996). To study the effect of the distance

266 from the road to the slope, the annual risk to different types of vehicles and persons along Kennedy

267 Road are calculated as the distance between the slope and the road varies, and the results are shown

268 in Figure 11. As can be seen from this figure, the annual risk to vehicles along Kennedy Road is

269 reduced as l_{th} becomes larger. When $l_{th} / H = 0.7$, the risk is reduced by half compared the case of $l_{th} /$

270 $H = 0.1$. When l_{th} / H is 2, the risk is negligible. Thus, increasing the distance between the slope and

271 the road can effectively reduce the risk of landslides.

272

273 4.3 Effect of traffic flow

What about weather conditions and their relationship to traffic flow and AFP?

274 As can be seen from Fig. 7, since the number of vehicles during different periods in a day is different,

275 the mean rate of occurrence of vehicles in affected road due to the landslide is significantly different.

276 The high density of vehicles may pose a huge risk to vehicles and persons due to landslides. To



277 indicate the effect of density of vehicles on the landslide risk, the annual risk to all types of vehicles
278 and persons along Kennedy Road are investigated when the density of vehicles on the highway
279 increases from 0 to 300 vehicles per kilometer and the results are shown in Fig. 12. As can be seen
280 from this figure, there is a linear increasing trend of the annual risk to all types of vehicles and
281 persons as density of vehicles increases. When the density of vehicles is equal to 300 vehicles per
282 kilometer, the annual risk to vehicles and persons can reach 1.01×10^{-2} vehicles being hit per year
283 and 5.52×10^{-2} persons being hit per year, respectively. Therefore, the high density of vehicles will
284 significantly enhance the annual risk to vehicles and persons due to landslides and properly
285 managing transportation and ensuring smooth traffic flow are important to reduce the risk.

It is important to mention that the proposed model applicability is for back analysis of landslides, because you need information about landslide scar to estimate the volume and then L. Otherwise, you need to take into account more suppositions or to consider more uncertainties

287 **5 Summary and Conclusions**

288 Quantitative assessment the risk of vehicles hit by landslides can help better understand and manage
289 such kind of risk. Using a case study in Hong Kong, this paper suggests a method to assess the risk
290 of highway landslide. For the slope studied in this paper, the annual failure probability is first
291 assessed based on historical slope failure data in Hong Kong. The spatial impact of the landslide is
292 then analyzed using an empirical ^{runout} round out analysis method. The consequence of the landslide is ^{on vehicles}
293 assessed by modeling the traffic on the highway as a Poisson process. For the slope examined in this
294 paper, it is found that different types of vehicles may be associated with different levels of risk. Also,
295 it is found that the annual failure probability of the slope, the distance from the slope and the road
296 and the density of vehicles on the road can significantly affect the landslide risk and the suggested
297 method can be used to quantify the effect of the above factors. The suggested method can also be
298 potentially used to analyze the highway landslide risk in other regions.

Of course, but with which adjustments or considerations?

I think that a good contribution of your research can be to establish new guidelines for highways design for purposes of roadway safety in terms of landslide risk reduction hitting vehicles & persons. For this, the methodology can be more detailed looking for include some uncertainties involve in the process providing innovative or novelty processes or methods.



299

300 **Acknowledgements**

301 This research was substantially supported by the National Key Research and Development Program
302 of China (2018YFC0809600, 2018YFC0809601), the National Natural Science Foundation of China
303 (41672276, 51538009), the Key Innovation Team Program of MOST of China (2016RA4059), and
304 Fundamental Research Funds for the Central Universities.

305

306 **References**

307 Bíl, M., Vodák, R., Kubeček, J., Bílová, M., and Sedoník, J.: Evaluating road network damage
308 caused by natural disasters in the czech republic between 1997 and 2010, *Transportation Research*
309 *Part A*, 80, 90–103, 2015.

310 Budetta, P., and Riso, R. D.: The mobility of some debris flows in pyroclastic deposits of the
311 northwestern Campanian region (southern Italy), *Bulletin of Engineering Geology and the*
312 *Environment*, 63, 293–302, 2004.

313 Brand, E.W.: Landslides in Southeast Asia: A State-of-the-art Report, in: *Proceedings of the 4th*
314 *International Symposium on Landslides*, Toronto, Vol. 1, pp. 17–59, 1984.

315 Budetta, P.: Assessment of rockfall risk along roads, *Natural Hazards and Earth System Sciences*, 4,
316 71–81, 2004.

317 Christian, J. T., Ladd, C. C., and Baecher, G. B.: Reliability applied to slope stability analysis,
318 *Journal of Geotechnical Engineering*, ASCE, 120, 2180–2207, 1994.

319 Chau, K. T., Sze, Y. L., Fung, M. K., Wong, W. Y., Fong, E. L., and Chan, L. C. P.: Landslide hazard
320 analysis for Hong Kong using landslide inventory and GIS, *Computers and Geosciences*, 30,
321 429–443, 2004.



- 322 Cheung, R. W. M., and Tang, W. H.: Realistic assessment of slope reliability for effective landslide
323 hazard management, *Geotechnique*, 55, 85–94, 2005.
- 324 Corominas, J.: The angle of reach as a mobility index for small and large landslides, *Canadian*
325 *Geotechnical Journal*, 33, 260–271, 1996.
- 326 Donnini, M., Napolitano, E., Salvati, P., Ardizzone, F., Bucci, F., and Fiorucci, F., et al.: Impact of
327 event landslides on road networks: a statistical analysis of two Italian case studies, *Landslides*, 14,
328 1–15, 2017.
- 329 Dai, F. C., Lee, C. F., and Ngai, Y. Y.: Landslide risk assessment and management: an overview,
330 *Engineering Geology*, 64, 65–87, 2002.
- 331 Dorren, L., Sandri, A., Raetzo, H., and Arnold, P.: Landslide risk mapping for the entire Swiss
332 national road network, in: Malet, J. P., Remaître, A., and Bogaard, T. (Eds.), *Landslide Processes:*
333 *From Geomorphologic Mapping to Dynamic Modelling*, Utrecht University and University of
334 Strasbourg, Strasbourg, pp. 6–7, 2009.
- 335 Dai, F., and Lee, C.: Landslide characteristics and slope instability modeling using GIS, Lantau
336 Island, Hong Kong, *Geomorphology*, 42, 213–228, 2002.
- 337 Erener, A.: A regional scale quantitative risk assessment for landslides: Case of kumluca watershed in
338 Bartın, Turkey, *Landslides*, 10, 55–73, 2012.
- 339 Fenton, G. A., and Griffiths, D. V.: A slope stability reliability model, in: *Proceeding of the K.Y. Lo*
340 *Symposium (on CD)*, London, Ontario, 2005.
- 341 Finlay, P. J., Mostyn, G. R., and Fell, R.: Landslide risk assessment: prediction of travel distance,
342 *Canadian Geotechnical Journal*, 36, 556–562, 1999.
- 343 Fell, R., Ho, K. K. S., Lacasse, S., and Leroi, E.: A framework for landslide risk assessment and
344 management, in: Hungr, O., Fell, R., Couture, R., and Eberhardt, E. (Eds.), *Landslide Risk*
345 *Management*, Taylor and Francis, London, pp. 3–26, 2005.



- 346 Fell, R.: Landslide risk assessment and acceptable risk, *Canadian Geotechnical Journal*, 31, 261–272,
347 1994.
- 348 GovHK: Hong Kong—the Facts, Retrieved from www.gov.hk, 2019.
- 349 Gao, L., Zhang, L. M., and Chen, H. X.: Likely scenarios of natural terrain shallow slope failures on
350 Hong Kong Island under extreme storms, *Natural Hazards Review*, 18, B4015001, 2017.
- 351 GEO (Geotechnical Engineering Office): Highway slope manual, Civil Engineering and
352 Development Dept., Government of Hong Kong SAR, Hong Kong, 2017.
- 353 GEO (Geotechnical Engineering Office): Investigation of some major slope failures between 1992
354 and 1995, Civil Engineering and Development Dept., Government of Hong Kong SAR, Hong
355 Kong, 1996.
- 356 Guzzetti, F., Ardizzone, F., Cardinali, M., Galli, M., Reichenbach, P., and Rossi, M.: Distribution of
357 landslides in the Upper Tiber River basin, central Italy, *Geomorphology*, 96, 105–122, 2008.
- 358 Guzzetti, F., Ardizzone, F., Cardinali, M., Rossi, M., and Valigi, D.: Landslide volumes and landslide
359 mobilization rates in Umbria, central Italy, *Earth and Planetary Science Letters*, 279, 0–229, 2009.
- 360 Huang, J., Griffiths, D. V., and Fenton, G. A.: System reliability of slopes by RFEM, *Soils and*
361 *Foundations*, 50, 343–353, 2010.
- 362 Hosking, J. R. M., Wallis, J. R., and Wood, E. F.: Estimation of the generalized extreme-value
363 distribution by the method of probability-weighted moments, *Technometrics*, 27, 251–261, 1985.
- 364 Hungr, O., and McDougall, S.: Two numerical models for landslide dynamic analysis, *Computers*
365 *and Geosciences*, 35, 978–992, 2009.
- 366 Hungr, O., Corominas, J., and Eberhardt, E.: Estimating landslide motion mechanism, travel distance
367 and velocity, in: Hungr, O., Fell, R., Couture, R., and Eberhardt, E. (Eds.), *Landslide Risk*
368 *Management*, Taylor and Francis, London, pp. 99–128, 2005.
- 369 HKO (Hong Kong Observatory): Climate Statistics, Retrieved from www.hko.gov.hk, 2018.



- 370 Imaizumi, F., and Sidle, R. C.: Linkage of sediment supply and transport processes in Miyagawa
371 Dam catchment, Japan, *Journal Geophysical Research*, 112, F03012, 2007.
- 372 Lessing, P., Messina, C. P., and Fonner, R. F.: Landslide risk assessment. *Environmental Geology*, 5,
373 93–99, 1983.
- 374 Luo, H. Y., Zhang, L. L., and Zhang, L. M.: Progressive failure of buildings under landslide impact,
375 *Landslides*, 16, 1327–1340, 2019.
- 376 Lighthill, M., J.: On kinematic waves ii. a theory of traffic flow on long crowded roads, *Proceedings*
377 *of the Royal Society, A Mathematical Physical & Engineering Sciences*, 229, 317–345, 1955.
- 378 Lumb, P.: Slope failures in Hong Kong. *Quarterly Journal of Geology*, 8, 31–65, 1975.
- 379 Michoud, C., Derron, M. H., Horton, P., Jaboyedoff, M., Baillifard, F. J., Loye, A., Nicolet, P.,
380 Pedrazzini, A., and Queyrel, A.: Rockfall hazard and risk assessments along roads at a regional
381 scale: example in Swiss Alps, *Natural Hazards and Earth System Sciences*, 12, 615–629, 2012.
- 382 Malamud, B. D., Turcotte, D. L., Guzzetti, F., and Reichenbach, P.: Landslide inventories and their
383 statistical properties. *Earth Surface Processes and Landforms*, 29, 687–711, 2004.
- 384 Nicolet, P., Jaboyedoff, M., Cloutier, C., Crosta, G. B., and Lévy, S.: Brief communication: on direct
385 impact probability of landslides on vehicles, *Natural Hazards and Earth System Sciences*, 16,
386 995–1004, 2016.
- 387 Negi, I. S., Kumar, K., Kathait, A., and Prasad, P. S.: Cost assessment of losses due to recent
388 reactivation of Kaliasaur landslide on National Highway 58 in Garhwal Himalaya, *Natural*
389 *Hazards*, 68, 901–914, 2013.
- 390 Paxson, V., and Floyd, S.: Wide-area traffic: The failure of Poisson modeling, *IEEE/ACM*
391 *Transactions on Networking*, 3, 226–244, 1995.
- 392 Parker, R. N., Densmore, A. L., Rosser, N. J., De Michele, M., Li, Y., and Huang, R., et al.: Mass
393 wasting triggered by the 2008 Wenchuan earthquake is greater than orogenic growth, *Nature*
394 *Geoscience*, 4, 449–452, 2011.



- 395 Peila, D., and Guardini, C.: Use of the event tree to assess the risk reduction obtained from rockfall
396 protection devices, *Natural Hazards and Earth System Sciences*, 8, 1441–1450, 2008.
- 397 Remondo, J., Bonachea, J., and Cendrero, A.: Quantitative landslide risk assessment and mapping on
398 the basis of recent occurrences, *Geomorphology*, 94, 496–507, 2008.
- 399 Scheidegger, A. E.: On the prediction of the reach and velocity of catastrophic landslides, *Rock*
400 *Mechanics and Rock Engineering*, 5, 231–236, 1973.
- 401 Transport Department of Hong Kong (TDHK): Transport in Hong Kong, Retrieved from
402 www.td.gov.hk, 2018.
- 403 Vega, J. A., and Hidalgo, C. A.: Quantitative risk assessment of landslides triggered by earthquakes
404 and rainfall based on direct costs of urban buildings, *Geomorphology*, 273, 217–235, 2016.
- 405 Zhang, J., and Tang, W. H.: Study of time-dependent reliability of old man-made slopes considering
406 model uncertainty, *Georisk: Assessment and Management of Risk for Engineered Systems and*
407 *Geohazards*, 3, 106–113, 2009.
- 408



409 **List of Tables**

410

411 **Table 1.** Percent, length and passenger capacity of vehicles in Hong Kong

412 **Table 2.** Number of vehicles passing a given cross section of road per hour and average speed of
413 vehicles on Kennedy Road in a day

414

415 **List of Figures**

416

417 **Figure 1.** Location of the landslide studied in this paper (© Google Maps 2019)

418 **Figure 2.** Typical cross section of the slope studied in this paper

419 **Figure 3.** Plan view of the slope studied in this paper

420 **Figure 4.** Histogram and fitted PDF of yearly maximum i_{24} in Hong Kong

421 **Figure 5.** CDF of yearly maximum i_{24} in Hong Kong

422 **Figure 6.** PDF of travel distance of the landslide studied in this paper

423 **Figure 7.** Mean rates of different types of vehicles during different periods: (a) morning peak (b)
424 normal period (c) evening peak. (1. Private buses, 2. Non-franchised public buses, 3.
425 Franchised buses, 4. Taxis, 5. Private cars, 6. Public light buses, 7. Private light buses, 8.
426 Goods vehicles, 9. Special purpose vehicles, 10. Government vehicles, 11. Motor cycles)

427 **Figure 8.** Probability distribution of number of private cars hit by the landslide studied in this
428 paper during different periods for the case of $\alpha_j(\mathbf{S} = \mathbf{S}_i) = 1$: (a) morning peak (b) normal
429 period (c) evening peak (d) considering uncertainty of failure time

430 **Figure 9.** Annual risk of elements hit by the landslide studied in this paper: (a) vehicles (b)
431 persons. (1. Private buses, 2. Non-franchised public buses, 3. Franchised buses, 4. Taxis,
432 5. Private cars, 6. Public light buses, 7. Private light buses, 8. Goods vehicles, 9. Special
433 purpose vehicles, 10. Government vehicles, 11. Motor cycles, 12. All types of vehicles)

434 **Figure 10.** Impact of failure probability of the slope on the landslide risk

435 **Figure 11.** Impact of distance between the landslide and the road on the landslide risk

436 **Figure 12.** Impact of density of vehicles on the landslide risk

437



438
439

Table 1. Percent, length and passenger capacity of vehicles in Hong Kong

Vehicles types	Percent (%)	Length (m)	Passenger capacity (persons)
Private buses	0.08	10	55
Non-franchised public buses	0.82	10	55
Franchised buses	0.72	10	55
Taxis	2.30	5	5
Private cars	71.41	5	5
Public light buses	0.50	9	33
Private light buses	0.39	9	33
Goods vehicles	13.77	12	2
Special purpose vehicles	0.23	5	1
Government vehicles	0.74	5	5
Motor cycles	9.24	2	1

440



441 Table 2. Number of vehicles passing a given cross section of road per hour and average speed of
442 vehicles on Kennedy Road in a day
443

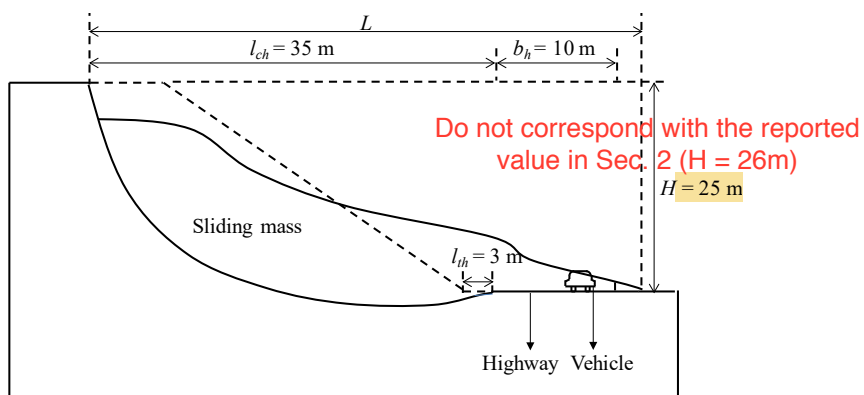
Periods in a day	Morning peak (7–9 am)	Normal period	Evening peak (5–7 pm)
q (vehicles per hour)	3000	1500	2800
v (km per hour)	15	30	15

444



445
446
447
448

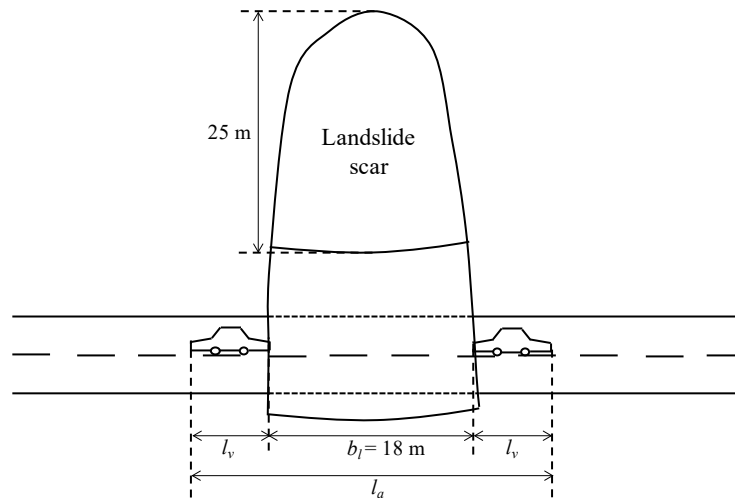
Figure 1. Location of the landslide studied in this paper (© Google Maps 2019)
It is suggested a convenient figure, preferably with own authorship.
As the figure is, it is not recommended for a scientific publication.



449
450
451
452

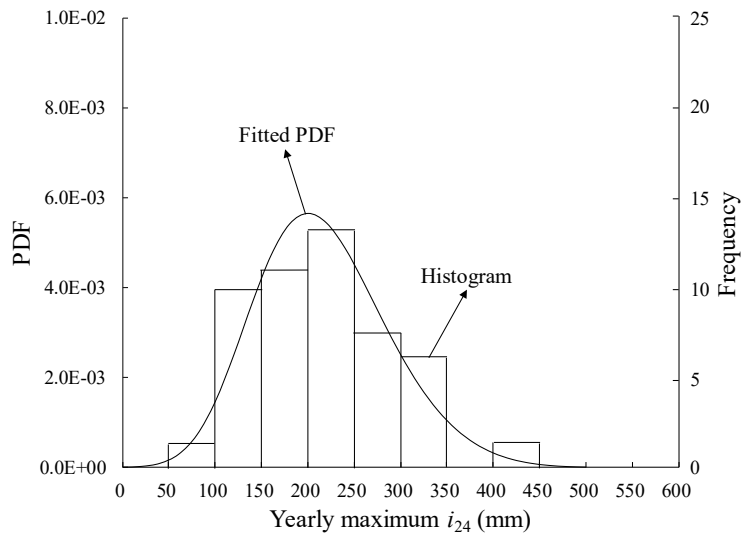
Figure 2. Typical cross section of the slope studied in this paper

It is suggested a better figure.
As the figure is, it is not proper for a scientific publication.



453
454
455
456

Figure 3. Plan view of the slope studied in this paper
It is suggested a better figure.
As the figure is, it is not proper for a scientific publication.



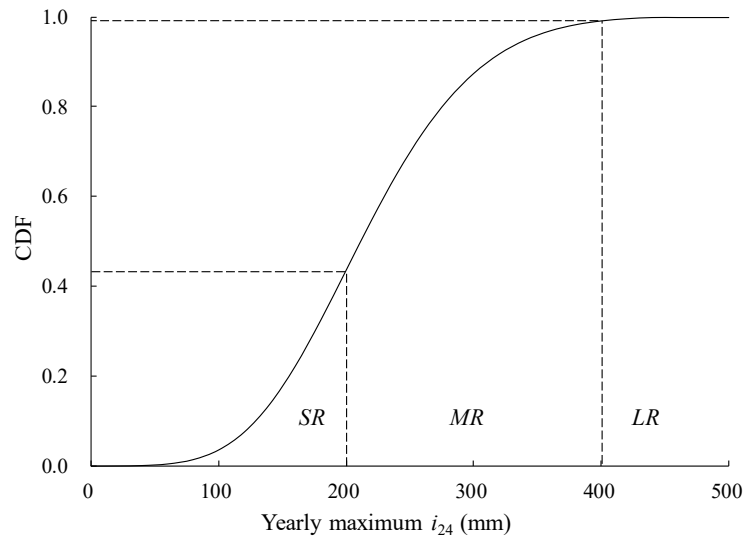
457

458

459

Figure 4. Histogram and fitted PDF of yearly maximum i_{24} in Hong Kong

460



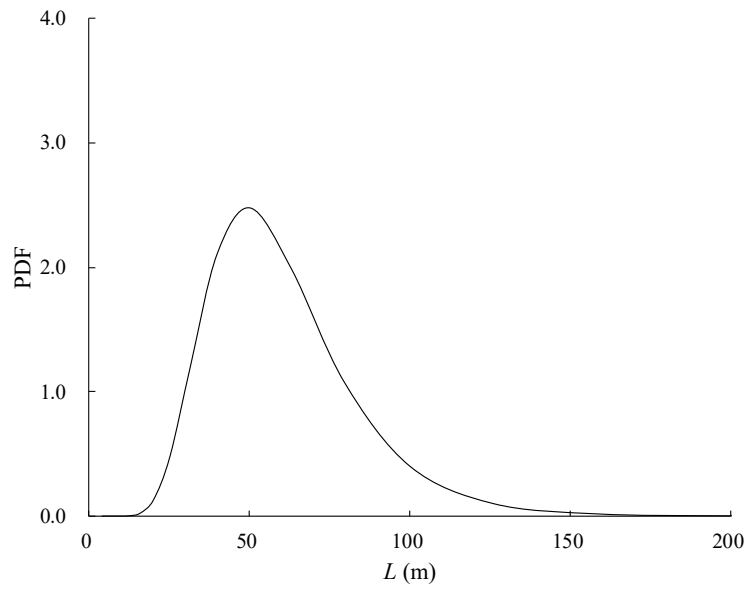
461

462

463

Figure 5. CDF of yearly maximum i_{24} in Hong Kong

464



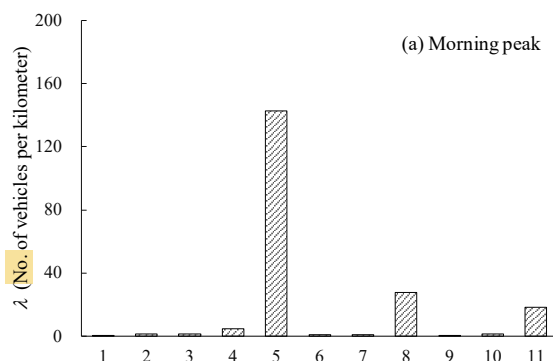
465
466
467
468

Figure 6. PDF of travel distance of the landslide studied in this paper

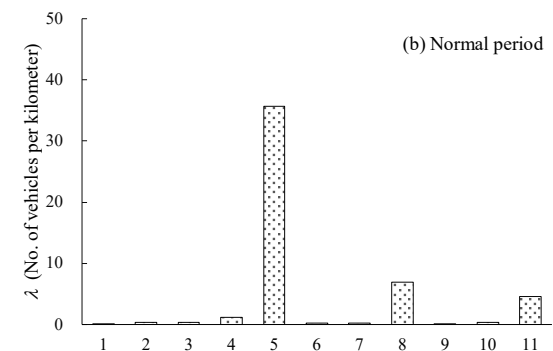


This is not the
adequate
symbol

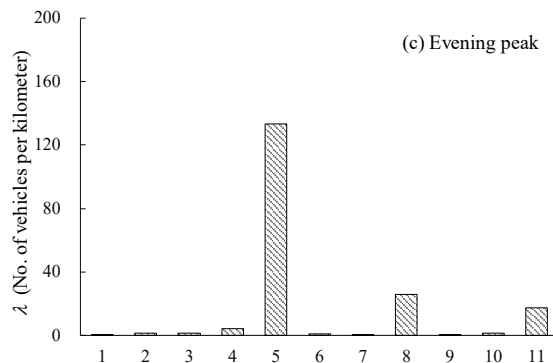
469



470

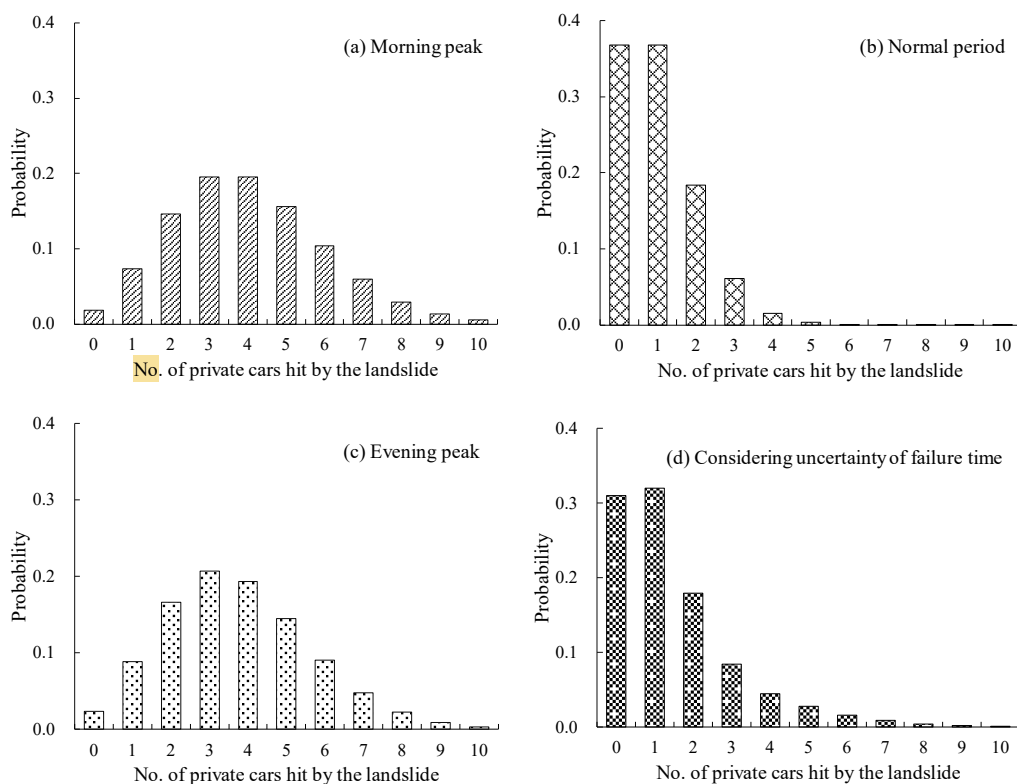


471



472

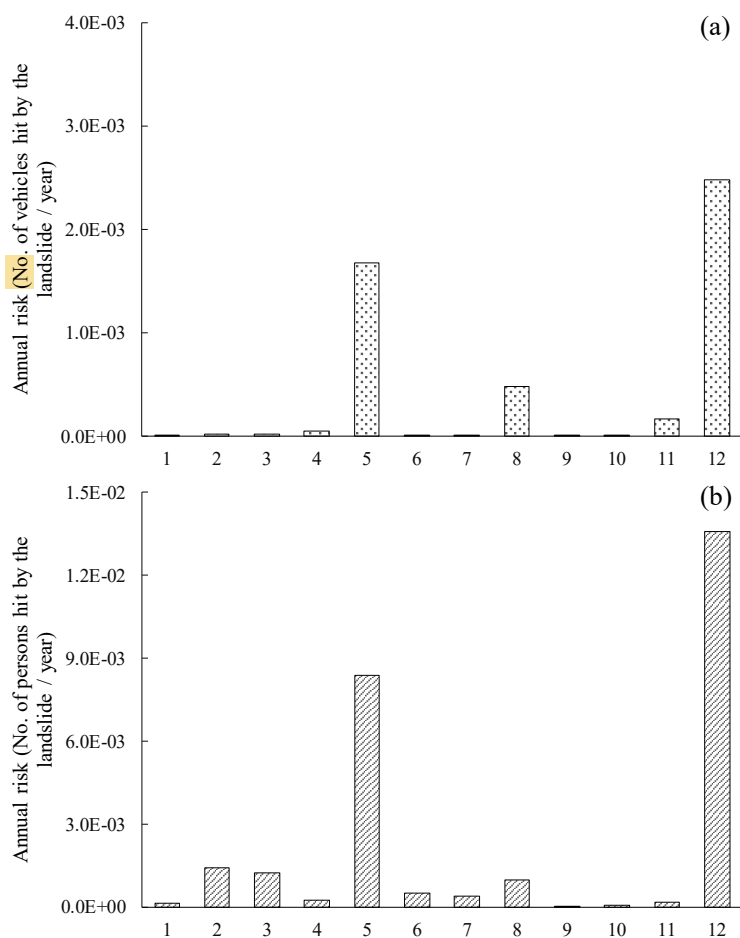
473 Figure 7. Mean rates of different types of vehicles during different periods: (a) morning peak (b)
474 normal period (c) evening peak. (1. Private buses, 2. Non-franchised public buses, 3. Franchised
475 buses, 4. Taxis, 5. Private cars, 6. Public light buses, 7. Private light buses, 8. Goods vehicles, 9.
476 Special purpose vehicles, 10. Government vehicles, 11. Motor cycles)



477
 478 Figure 8. Probability distribution of number of private cars hit by the landslide studied in this paper
 479 during different periods for the case of $\alpha_j(S = S_i) = 1$: (a) morning peak (b) normal period (c) evening
 480 peak (d) considering uncertainty of failure time
 481



482

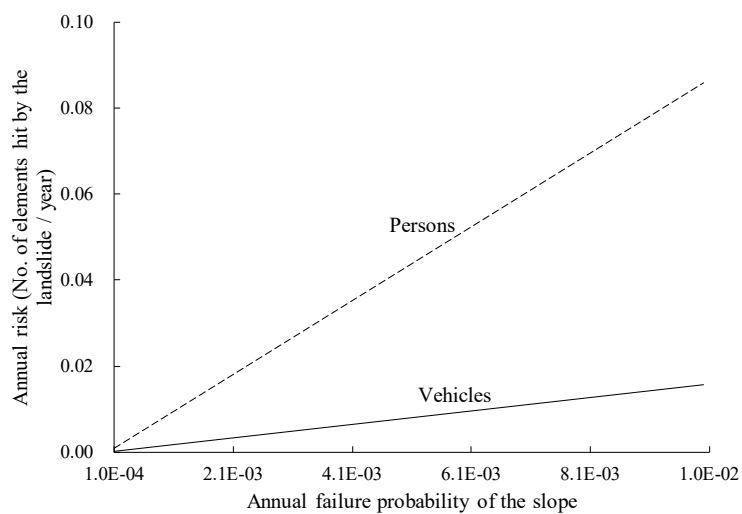


483

484

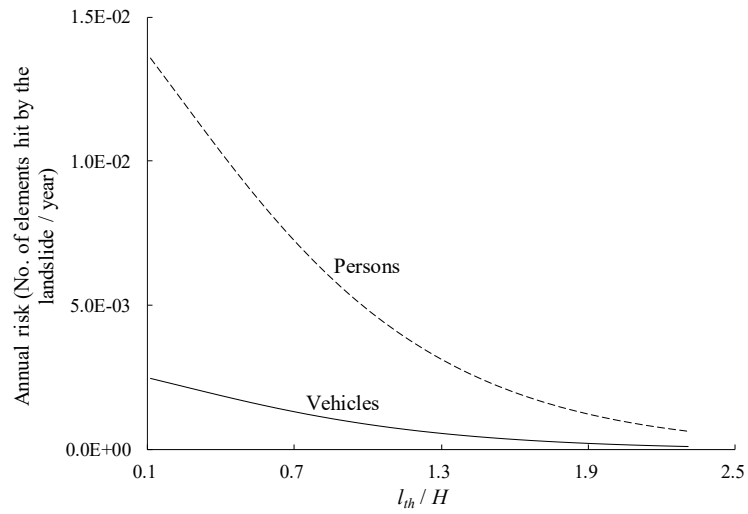
485 Figure 9. Annual risk of elements hit by the landslide studied in this paper: (a) vehicles (b) persons.
486 (1. Private buses, 2. Non-franchised public buses, 3. Franchised buses, 4. Taxis, 5. Private cars, 6.
487 Public light buses, 7. Private light buses, 8. Goods vehicles, 9. Special purpose vehicles, 10.
488 Government vehicles, 11. Motor cycles, 12. All types of vehicles)

489



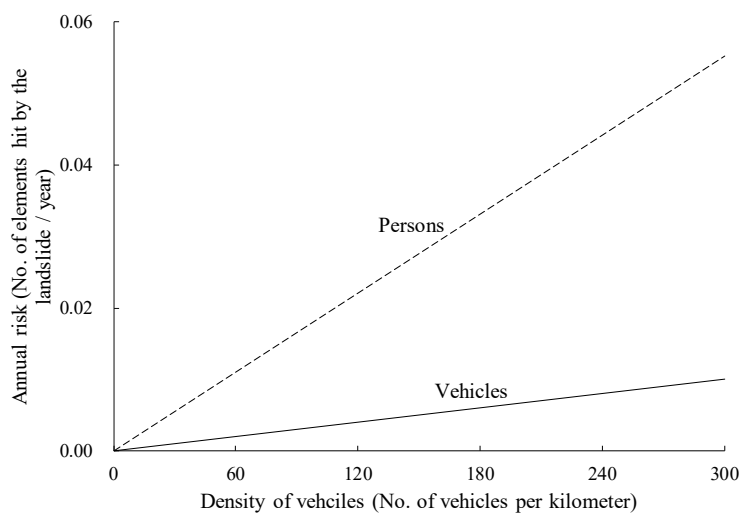
490
491
492
493

Figure 10. Impact of failure probability of the slope on the landslide risk



494
495
496
497

Figure 11. Impact of distance between the landslide and the road on the landslide risk



498
499
500

Figure 12. Impact of density of vehicles on the landslide risk